

Mean free paths and in-medium scattering cross sections of energetic nucleons in neutron-rich nucleonic matter within the relativistic impulse approximation

Wei-Zhou Jiang^{1,2}, Bao-An Li¹, and Lie-Wen Chen^{1,3}

¹ *Department of Physics, Texas A&M University-Commerce, Commerce, TX 75429, USA*

² *Institute of Applied Physics, Chinese Academy of Sciences, Shanghai 201800, China*

³ *Institute of Theoretical Physics, Shanghai Jiao Tong University, Shanghai 200240, China*

The mean free paths and in-medium scattering cross sections of energetic nucleons in neutron-rich nucleonic matter are investigated using the nucleon optical potential obtained within the relativistic impulse approximation with the empirical nucleon-nucleon scattering amplitudes and the nuclear densities obtained in the relativistic mean field model. It is found that the isospin-splitting of nucleon mean free paths, sensitive to the imaginary part of the symmetry potential, changes its sign at certain high kinetic energy. The in-medium nucleon-nucleon cross sections are analytically and numerically demonstrated to be essentially independent of the isospin asymmetry of the medium and increase linearly with density in the high energy region where the relativistic impulse approximation is applicable.

PACS numbers: 21.65.+f, 24.10.Ht, 24.10.Jv

I. INTRODUCTION

The in-medium nucleon-nucleon (NN) cross sections and the associated nucleon mean free paths (MFP) in neutron-rich nucleonic matter are important for understanding both the structure of rare isotopes and the reaction dynamics involving these nuclei. For instance, much information about the size of neutron skins and nucleon density profiles of neutron-rich nuclei can be obtained from Glauber model analyses of the total reaction cross sections[1]. A key input in these analyses is the isospin dependent in-medium NN cross sections. Usually, however, in most Glauber calculations only the isospin averaged free-space nucleon-nucleon cross section is used. The knowledge about the in-medium NN cross sections in neutron-rich matter will thus affect significantly the extracted structure information about rare isotopes. It is also critical for understanding nuclear reactions as the in-medium NN cross sections determine the stopping power and generally transport properties of nuclear matter. The in-medium NN cross sections, as basic inputs of transport models, are important in determining essentially all dynamical observables, such as, the collective flows, isospin diffusion, energy and momentum transfers, and particle production [2–7]. While the in-medium NN cross sections and the nuclear equation of state (EOS) are in principle determined by the same nuclear effective interaction, although they are sensitive to different parts and ranges of the interaction in the medium at different densities, much more attention has been putting on investigating the EOS than on the in-medium NN cross sections in neutron-rich matter. However, it was demonstrated recently that the major theoretical uncertainty in extracting the density dependence of the symmetry energy

of neutron-rich matter from heavy-ion reactions is our poor knowledge about the isospin-dependent in-medium NN cross sections[3]. It is encouraging to notice that more work is being done recently in calculating the in-medium NN cross sections using various approaches, such as, the relativistic and non-relativistic Brueckner theory [5, 8–16] and the Green function approach [17–19]. Nevertheless, most of these calculations are for in-medium NN cross sections in symmetric nuclear matter. Very little information is available for the isospin dependence of the NN cross section in neutron-rich matter. While the available calculations are indeed very useful, necessarily are the NN cross sections and the EOS consistently calculated using the same nuclear effective interactions.

The nucleon-nucleus optical potential plays a central role in determining the in-medium NN cross sections and the nucleon MFP. In particular, the imaginary part of the optical potential allows one to extract easily the MFP and thus also the in-medium NN cross sections. There are several possible ways to derive the optical potential [20]. It can be calculated from various models either non-relativistically or relativistically, with the microscopic Brueckner approach, see, e.g., Ref.[10, 12, 13, 21, 22]. Theoretically, approximations have to be made to render the calculations feasible. For instance, the evaluation of the imaginary part of the optical potential depends on the treatment of the widths of intermediate states that are rather unclear or the nucleon polarization in the medium that is in principle coupled to the vacuum. On the other hand, one can start from a physically reasonable approximation for the optical potential and determine its parameters using the experimental data [23]. The relativistic impulse approximation (RIA) actually follows this way. In the RIA, the optical potential is obtained in a form similar to the non-relativistic $t\rho$ approximation. Within the RIA, the basic ingredients of the optical potential are the free Lorentz invariant NN scattering amplitudes and the nuclear scalar and vector densities in nuclear matter [24–28]. An attractive feature of the RIA is that the relativistic optical potentials are experimentally constrained by the free-space NN scattering data. The nuclear densities are calculated from the relativistic mean-field (RMF) models that provide also a dynamical description for the spin-orbit coupling [29]. Along with the success of the RMF models in describing the nuclear structure, the RIA was justified by nicely reproducing the proton-nucleus elastic scattering data at high energies. Of course, the limitation of the RIA is that it is valid only at reasonably high energies in not so dense matter. As most of the existing microscopic calculations were devoted to the low and intermediate energy regions, the in-medium NN cross sections at high energies remain largely unknown. Our study here of the nucleon MFP and in-medium NN cross sections at high energies within the RIA is thus complementary to the existing work. Moreover, given the exciting scientific opportunities provided by the constructions of several high energy radioactive beam facilities around the world, the knowledge on the mean free paths and in-medium scattering cross sections of energetic nucleons in neutron-rich nucleonic matter

is certainly necessary and useful.

The paper is organized as follows. In section II, the main formulas of the RMF, RIA, and the calculations of the nucleon MFP's and in-medium NN cross sections are briefly reviewed. The results and discussions are presented in section III. Finally, a summary is given in Section IV.

II. A BRIEF SUMMARY OF THE FORMALISM

In the present work, we use the relativistic model Lagrangian [30]

$$\begin{aligned} \mathcal{L} = & \bar{\psi}[i\gamma_\mu\partial^\mu - M + g_\sigma^*\sigma - g_\omega^*\gamma_\mu\omega^\mu - g_\rho^*\gamma_\mu\tau_3b_0^\mu - e\frac{1}{2}(1 + \tau_3)\gamma_\mu A^\mu]\psi + \frac{1}{2}(\partial_\mu\sigma\partial^\mu\sigma - m_\sigma^{*2}\sigma^2) \\ & - \frac{1}{4}F_{\mu\nu}F^{\mu\nu} + \frac{1}{2}m_\omega^{*2}\omega_\mu\omega^\mu - \frac{1}{4}B_{\mu\nu}B^{\mu\nu} + \frac{1}{2}m_\rho^{*2}b_{0\mu}b_0^\mu - \frac{1}{4}A_{\mu\nu}A^{\mu\nu}, \end{aligned} \quad (1)$$

where ψ, σ, ω , and b_0 are the fields of the nucleon, scalar, vector, and isovector-vector mesons, with their masses $M, m_\sigma^*, m_\omega^*$, and m_ρ^* , respectively. The meson coupling constants and masses with asterisks denote the density dependence, and they are given by the BR scaling [30–32]. The Dirac spinor in momentum space is written as

$$\psi(k) = \sqrt{\frac{E^* + M^*}{2E^*}} \begin{pmatrix} 1 \\ \frac{\sigma \cdot \mathbf{k}}{E^* + M^*} \end{pmatrix} \chi_s, \quad (2)$$

with $M^* = M - g_\sigma^*\sigma$, $E^* = \sqrt{M^{*2} + \mathbf{k}^2}$, and χ_s the Pauli spinor. The (0th-component) vector and scalar densities are respectively give by

$$\rho_{B,i} = \int_0^{k_{F,i}} \frac{d^3k}{(2\pi)^3} \psi^\dagger(k)\psi(k) = \frac{1}{3\pi^2} k_{F,i}^3 \quad (3)$$

$$\rho_{s,i} = \int_0^{k_{F,i}} \frac{d^3k}{(2\pi)^3} \psi^\dagger(k)\gamma_0\psi(k) = \int_0^{k_{F,i}} \frac{d^3k}{(2\pi)^3} \frac{M^*}{E^*}, \quad (4)$$

with $i = p, n$. With Dirac spinors, the NN scattering amplitudes can be defined [28]. The Lorentz invariant NN scattering amplitude can be decomposed into five components

$$\mathcal{F} = F_S + F_V\gamma_1^\mu\gamma_{2\mu} + F_T\sigma_1^{\mu\nu}\sigma_{2\mu\nu} + F_P\gamma_1^5\gamma_2^5 + F_A\gamma_1^5\gamma_1^\mu\gamma_2^5\gamma_2^\mu, \quad (5)$$

where S,V,T,P and A denote the scalar, vector, tensor, pseudoscalar and axial vector, respectively. The five components are dependent on the squared momentum transfer \mathbf{q}^2 . The scattering amplitude in the RIA is obtained from the expectation value of a sum of single two-body NN scatterings. For the spin-saturated nucleus, only survived are the scalar (F_S), vector (F_V) and tensor (F_T) terms, while the scalar and vector parts dominate the scattering amplitude. In the RIA, the optical potential in momentum space is thus the sum of the products of the density and amplitude of respective scalar and vector components [24, 25]

$$\tilde{U}_{opt}(\mathbf{q}) = -\frac{4\pi i p_{lab}}{M} [F_S(\mathbf{q})\tilde{\rho}_S(\mathbf{q}) + \gamma_0 F_V(\mathbf{q})\tilde{\rho}_B(\mathbf{q})], \quad (6)$$

where p_{lab} and M are the laboratory momentum and mass of the incident nucleon, respectively. This expression is similar to the $t\rho$ approximation in the non-relativistic approximation. The momentum dependence of the optical potential can give details of the angular distribution of nucleon scatterings, while the total cross section depends only on the forward scattering where $\mathbf{q} = 0$. Following Ref. [33], here we are interested in the optical potential in nuclear matter where the densities in coordinate space are constant. This means that a delta function $\delta(\mathbf{q})$ is induced so that $\mathbf{q} = 0$ in the scattering amplitudes in Eq.(5). Therefore the optical potential in nuclear matter in coordinate space is given as:

$$U_{opt} = -\frac{4\pi i p_{lab}}{M} [F_S \rho_S + \gamma_0 F_V \rho_B], \quad (7)$$

where ρ_S and ρ_B are the spatial scalar and vector densities of nucleons, respectively. For the application to the scattering on finite nuclei, one can resort to the local density approximation. Similar to Ref. [33], here we adopt the F_S and F_V determined directly from the experimental NN phase shifts [28]. The optical potential is decomposed into the following form

$$U_{opt} = U_S^{tot} + \gamma_0 U_0^{tot}. \quad (8)$$

with U_S^{tot} and U_0^{tot} denoting, respectively, the scalar and (0th-component) vector parts of the optical potential. Since U_S^{tot} and U_0^{tot} are generally complex, they can be further expressed as

$$U_S^{tot} = U_S + iW_S, \quad U_0^{tot} = U_0 + iW_0. \quad (9)$$

An application of relativistic optical potentials is to evaluate the nucleon MFP based on the dispersion relation which in the relativistic frame is written as

$$(E_k - U_0^{tot})^2 = \mathbf{k}^2 + (M + U_S^{tot})^2. \quad (10)$$

Equivalently, it can be written in a form similar to the non-relativistic approximation [34]

$$\frac{k_\infty^2}{2M} = \frac{k^2}{2M} + U_{sep}^{tot}(E_{kin}), \quad (11)$$

where the Schrödinger equivalent potential (SEP) is given by

$$U_{sep}^{tot} = U_S^{tot} + U_0^{tot} + \frac{1}{2M} (U_S^{tot2} - U_0^{tot2}) + \frac{U_0^{tot}}{M} E_{kin}, \quad (12)$$

with $k_\infty^2 = E_{kin}^2 + 2ME_{kin}$, $E_k = E_{kin} + M$, and $U_{sep}^{tot} = U_{sep} + iW_{sep}$. The real part of the symmetry potential is

$$U_{sym} = \frac{U_{sep}^n - U_{sep}^p}{2\delta}, \quad (13)$$

with the isospin asymmetry $\delta = (\rho_n - \rho_p)/\rho_B$. The above U_{sym} taken at the normal density is the well known Lane potential extracted from nucleon-nucleus scatterings [35]. Similarly, we can define an imaginary symmetry potential as

$$W_{sym} = \frac{W_{sep}^n - W_{sep}^p}{2\delta}. \quad (14)$$

Using the dispersion relation (11) and assuming a complex momentum $k = k_R + ik_I$, the nucleon MFP λ is derived exactly as [36]

$$\lambda = \frac{1}{2k_I} = \frac{1}{2} \left[-M \left(E_{kin} + \frac{E_{kin}^2}{2M} - U_{sep} \right) + M \left(\left(E_{kin} + \frac{E_{kin}^2}{2M} - U_{sep} \right)^2 + W_{sep}^2 \right)^{1/2} \right]^{-1/2}. \quad (15)$$

A much simpler expression for the nucleon MFP can be derived by expanding the momentum in the vicinity of k_R [37]. The real and imaginary parts of the momentum is thus obtained as

$$k_R = (E_{kin}^2 + 2ME_{kin} - 2MU_{sep})^{1/2}, \quad k_I = -W_{sep} \left(\frac{k_R}{M} + \frac{\partial U_{sep}}{\partial k_R} \right)^{-1}. \quad (16)$$

Since there is no explicit momentum dependence in the optical potentials with the RIA, the nucleon MFP is written as

$$\lambda_i = \frac{1}{2k_I^i} = -\frac{k_R^i}{2MW_{sep}^i}, \quad i = p, n. \quad (17)$$

Numerically, we noted that almost the same nucleon MFP can be obtained from either Eq.(15) or (17), while the latter is more convenient for making analytical analyses. The nucleon MFP can also be measured as the length of the unit volume defined by the matter density and the NN cross section, and it is thus expressed by [38]

$$\lambda_i = (\rho_p \sigma_{ip}^* + \rho_n \sigma_{in}^*)^{-1}, \quad (18)$$

where ρ_p and ρ_n are respectively the proton and neutron densities. The in-medium NN cross sections can be obtained by inverting the above equation. To write the results compactly, we may define the following two quantities,

$$\tilde{\Lambda}^{-1} = \frac{1}{2} \left(\frac{1}{\lambda_n} + \frac{1}{\lambda_p} \right), \quad \tilde{\lambda}^{-1} = \frac{1}{2\delta} \left(\frac{1}{\lambda_n} - \frac{1}{\lambda_p} \right). \quad (19)$$

They can be further written in terms of the imaginary parts of the symmetry potential and the isoscalar SEP using Eqs.(14) and (17)

$$\tilde{\Lambda}^{-1} = \frac{2M}{k_R} \bar{W}_{sep}, \quad \tilde{\lambda}^{-1} = \frac{2M}{k_R} W_{sym}, \quad (20)$$

where the $k_R^{n,p}$ are approximated by the k_R . This is a very good approximation because at high energies the U_{sym} is negligible compared to the kinetic energy and the isoscalar SEP's given by

$$\bar{U}_{sep} = (U_{sep}^n + U_{sep}^p)/2, \quad \bar{W}_{sep} = (W_{sep}^n + W_{sep}^p)/2. \quad (21)$$

This point will be shown numerically in the next section. As it was pointed out in Ref. [33], the U_{sym} itself is isospin independent because the difference between the neutron and proton potentials is largely linear in isospin asymmetry. We find that such an isospin independence retains also for the W_{sym} . It is therefore understandable that the $\tilde{\Lambda}$ and $\tilde{\lambda}$ are essentially independent of the isospin asymmetry of the medium at high energies where the RIA is valid. Consequently, at these high energies the in-medium NN cross sections are also independent of the isospin asymmetry of the medium. Of course, there is still a difference between the neutron-proton and proton-proton (neutron-neutron) cross sections. In terms of these isospin independent quantities, the in-medium NN cross sections are obtained as

$$\sigma_{nn}^* = (\tilde{\Lambda}^{-1} + \tilde{\lambda}^{-1})/\rho_B, \quad \sigma_{np}^* = (\tilde{\Lambda}^{-1} - \tilde{\lambda}^{-1})/\rho_B. \quad (22)$$

Here we assume that $\sigma_{nn}^* = \sigma_{pp}^*$, thus neglecting the small charge symmetry breaking effect [39] and the isospin-dependent Pauli blocking effects in asymmetric nuclear medium. The neglect of the former is also consistent with the model Lagrangian we used in this work. We do not consider the tiny proton-neutron mass splitting in free space. Moreover, our model Lagrangian similar to those used in most other RMF models does not include the scalar-isovector δ meson responsible for the in-medium proton-neutron effective mass splitting. The same nn and pp scattering amplitudes are thus expected to result in the equal in-medium nn and pp cross sections. We stress here that the above results are only applicable to the high energy region where the RIA is valid and Pauli blocking effects are negligible. At low energies, the U_{sym} and isospin-dependent Pauli blocking effects are not negligible, and the resulting NN cross sections will depend on the isospin asymmetry of the medium.

III. RESULTS AND DISCUSSIONS

The RMF model used here is the SL1 we constructed in our previous work [30]. The scalar densities used in the RIA are calculated with the SL1. The scalar densities calculated at low densities ($\rho \leq 1.5\rho_0$) are quite similar with various models ranging from the best-fit models to the SL1. We refer the reader to our earlier work [30] for more details about the RMF with the SL1 parameter set.

A. Schrödinger equivalent potential

The proton and neutron SEP's obtained with the RIA serve as the basis to study the nucleon MFP and in-medium NN cross sections in this work. The isoscalar nucleon SEP, defined by the mean value of the neutron and proton SEP's in Eq. (21), is displayed in Fig. 1. It is seen that the imaginary SEP is stronger than the real one for nucleons at high kinetic energies. As the kinetic energy increases, the magnitude of the SEP increases very slowly. Consequently, this results in a

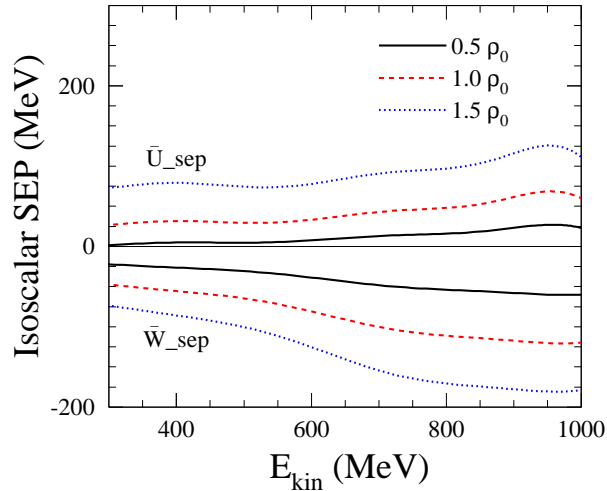


FIG. 1: (Color online) The isoscalar Schrödinger equivalent potential as a function of the nucleon kinetic energy for different densities.

correspondingly small decrease of the nucleon MFP, as given by Eq.(17). Shown in Fig. 2 are the real and imaginary parts of the symmetry potential, defined by Eqs.(13) and (14), respectively. Indeed, we find that these potentials are independent of the isospin asymmetry of the medium. For the U_{sym} , this was also found previously [33]. In Ref. [33], it was pointed out that the real part of the symmetry potential at fixed baryon densities is essentially a constant at high nucleon kinetic energies. As shown in the upper panel of Fig. 2, this is also true here. The U_{sym} is negligibly small, actually very close to zero, in the whole energy range considered. This finding is consistent with the tendency of the energy dependence of the Lane potential extracted from nucleon-nucleus scatterings, which indicates that the Lane potential decreases with the increasing incident energy up to about 100 MeV above which there is still no data[20]. The smallness of U_{sym} shown in the figure numerically justifies the approximation of using the k_R instead of the $k_R^{n,p}$ in Eq.(20). The imaginary part of the symmetry potential, which differentiates proton and neutron absorptions in nuclear medium, displays a different dependence on the kinetic energy from that for the U_{sym} . It is particularly interesting to note that its sign changes around $E_{kin} \approx 630 \text{ MeV}$ from positive to negative. This change can be reflected in the energy dependence of the nucleon MFP's.

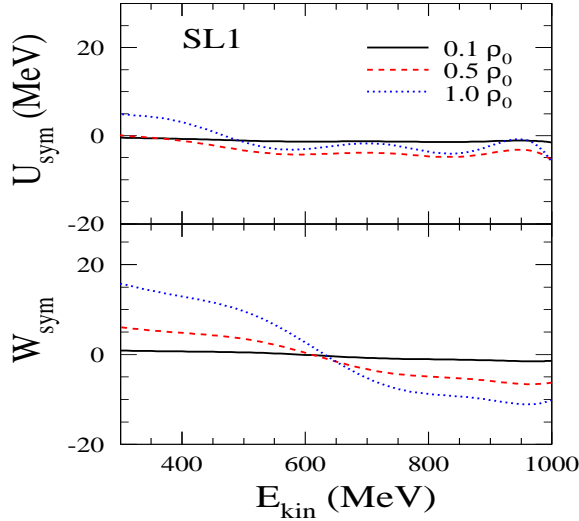


FIG. 2: (Color online) The symmetry potential as a function of the nucleon kinetic energy for different densities.

B. Nucleon mean free path

The nucleon MFP's, calculated from Eq.(15) or (17), are shown in Fig. 3. We find that at higher kinetic energies the nucleon MFP changes little with the energy and it is much less sensitive to the isospin asymmetry. The rapid change of the nucleon MFP occurs around $E_{kin} \approx 630\text{MeV}$. It is interesting to see that the isospin-splitting between the neutron and proton MFP changes at $E_{kin} \approx 630\text{MeV}$. The nucleon MFP is determined by both the real and imaginary parts of the SEP as seen in Eq.(17). The difference between the real parts of the neutron and proton SEP's is tiny compared to the nucleon momentum at high kinetic energies. In fact, we see from Fig. 2 that the real part, i.e., U_{sym} , is close to zero. Therefore, the change of the isospin-splitting between the neutron and proton MFP's can be attributed to the sign change of the imaginary part of the symmetry potential as shown in the lower panel of Fig. 2. This change for MFP's of neutrons and protons around 600 MeV/A may have interesting experimental consequences and certainly deserves further studies.

At $E_{kin} \geq 700$ MeV, the nucleon MFP is insensitive to the isospin asymmetry of the medium. This insensitivity is due to the fact that at high nucleon kinetic energies the W_{sym} , responsible for the difference between the proton and neutron MFP's, is small compared to the \bar{W}_{sep} that dominates the contributions to the nucleon MFP's. At lower kinetic energies, however, appreciable sensitivity to the isospin asymmetry exists just because the imaginary part of the symmetry potential is comparably

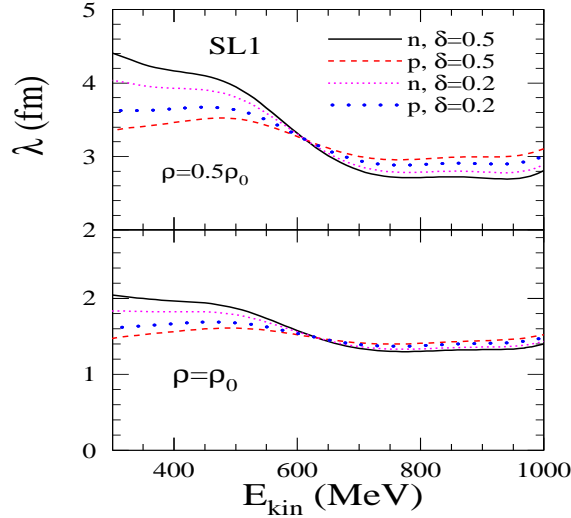


FIG. 3: (Color online) The nucleon mean free path as a function of the nucleon kinetic energy for different densities.

not so small. Comparing the two panels of Fig. 3, it is seen that the sensitivity of the nucleon MFP to the isospin asymmetry is reduced with the increasing density. This is also understandable because of the decreasing nucleon MFP's and the drop of the W_{sym} to \bar{W}_{sep} ratio at higher densities.

C. In-medium NN cross sections

As discussed briefly in the text below Eq.(20), in the energy range where the RIA is valid, the in-medium NN cross sections σ_{np}^* and $\sigma_{nn,pp}^*$ are independent of the isospin asymmetry of the medium. They depend only on the density and the nucleon kinetic energy. Before presenting our results, it is worthwhile to add some more discussions. Usually, the in-medium NN cross section relies on the isospin asymmetry at low kinetic energies. Such dependence is introduced by the isospin dependent nucleon SEP through the real part of the momentum k_R , given by Eq.(16). In the non-relativistic limit, it has $k_R^i = (2ME_{kin} - 2MU_{sep}^i)^{1/2}$ with $i = n, p$. The k_R^n and k_R^p can have considerable difference due to the non-negligible U_{sym} , which, for instance, can be found in Refs. [40, 41], at various isospin asymmetries. In fact, this is also related to the Pauli blocking which contributes a $\rho^{2/3}$ -dependence in the kinetic part of the symmetry energy [21, 42–45]. At low energies the different Pauli blocking for neutrons and protons in asymmetric matter are important. They can essentially lead to the dependence of the in-medium NN cross sections on the isospin asymmetry of the medium. In the energy region where RIA is valid, the kinetic energies are much higher (roughly above 400MeV)

with the relative nucleon momentum $k \gg k_F$. The Pauli blocking thus becomes irrelevant.

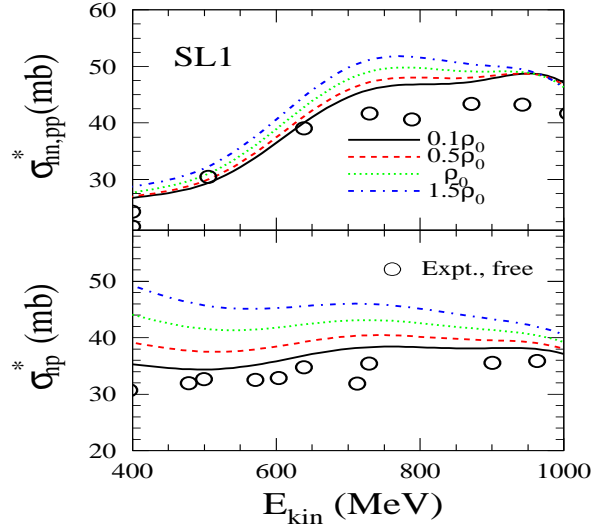


FIG. 4: (Color online) The in-medium NN cross sections as a function of the nucleon kinetic energy for different densities. The data for free NN cross sections are taken from Ref. [46].

The σ_{np}^* and $\sigma_{nn,pp}^*$ are calculated from the nucleon MFP's with Eqs.(19) and (22). As shown in Figs. 4 and 5, the in-medium NN cross sections increase with the density. At first glance, this feature seems to be in contrast to that occurring at lower energies where the Pauli blocking plays an important role in reducing the in-medium NN cross sections. However, at higher kinetic energies the in-medium NN cross sections are not necessarily constrained to be a descending function of density. In Fig. 4, as a check we see that the calculated NN cross sections at the very low density of $0.1\rho_0$ are very close to the free-space NN scattering data. Moreover, the in-medium NN cross sections are shown to be linear in density. This can be easily understood. As seen in Eqs.(20) and (22), the in-medium NN cross section are eventually determined by the SEP's which are quadratic in relativistic optical potentials, while the latter, given by Eq.(7), is linear in density. We note that the scalar density in Eq.(7) is linear in density in the relatively low density region where the RIA is applicable. Considering the density factor appearing in the denominator of Eq.(22), the in-medium NN cross section is therefore linearly proportional to the density. Interestingly, the ascending tendency of the in-medium cross section with density has also be seen at higher energies using some other approaches [7, 8, 10]. For instance, in Ref. [7], with the closed time path Green's function approach it was found that the $\sigma_{nn,pp}^*$ increases with density at $E_{kin} \geq 240$ MeV.

It is also seen in Figs. 4 and 5 that σ_{np}^* depends more strongly on the density than $\sigma_{nn,pp}^*$, while

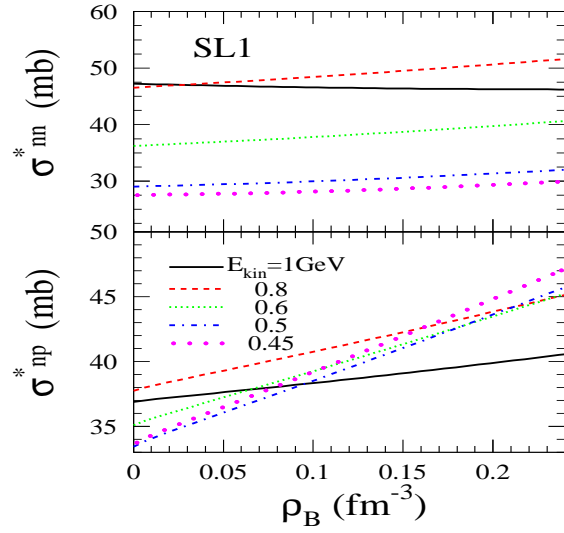


FIG. 5: (Color online) The in-medium NN cross sections as a function of the density for various kinetic energies.

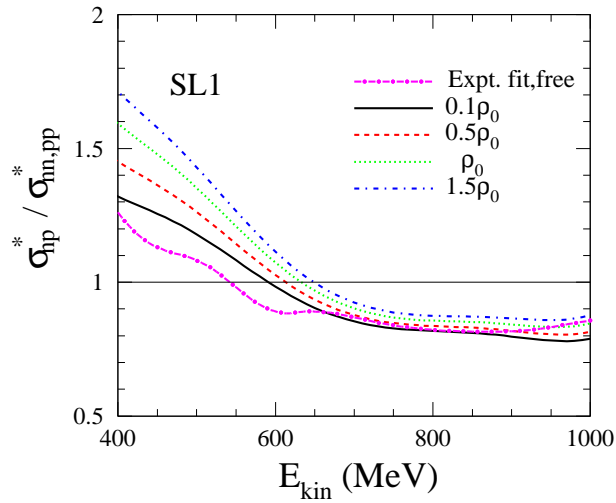


FIG. 6: (Color online) The ratio of σ_{np}^* to $\sigma_{nn,pp}^*$ for various densities.

the latter is more sensitive to the kinetic energy than the former. This different density and energy dependence for σ_{np}^* and $\sigma_{nn,pp}^*$ is actually a result of the distinction between the isovector ($T=1$) and isoscalar ($T=0$) interactions. Shown in Fig. 6 is the ratio $\sigma_{np}^*/\sigma_{nn,pp}^*$ as a function of nucleon kinetic energy. The ratio is an ascending function of density. This feature is also different from that at

low and intermediate energies. It is clearly shown that the magnitude of $\sigma_{nn,pp}^*$ exceeds σ_{np}^* around $E_{kin} \geq 600\text{MeV}$ depending on the density. For a comparison, the experimental value in free space is also shown in Fig. 6. The experimental $\sigma_{np}^*/\sigma_{nn,pp}^*$ ratio becomes smaller than 1 above about 580 MeV. The general trend is qualitatively consistent with the calculations in the medium at the low density limit. It is worth noting that the in-medium NN cross sections obtained in the RIA rely little on the phenomenological freedoms except for those in the RMF model to calculate the scalar density. In fact, within the density region we considered in this study the scalar densities are almost the same for the SL1 model and the best-fit models, such as, the FSUGold [48].

IV. SUMMARY

We have evaluated the relativistic optical potentials for neutrons and protons in asymmetric nuclear matter at high energies based on the relativistic impulse approximation with the empirical NN scattering amplitudes and the nuclear densities obtained in the relativistic mean field model. The Schrödinger equivalent potentials obtained from the relativistic optical potentials are then applied to calculate the nucleon mean free paths and the in-medium NN cross sections. The isospin-splitting of the proton and neutron mean free paths in asymmetric nuclear matter changes its sign at certain high energies, consistent with the changing sign of the underlying imaginary part of the symmetry potential. The small imaginary part of the symmetry potential at higher energies, compared to the counterpart of the isoscalar Schrödinger equivalent potential, accounts for the nucleon mean free paths with a much reduced sensitivity to the isospin asymmetry, while the negligibly small real part of the symmetry potential results in the in-medium NN cross sections independent of the isospin asymmetry of the medium. Moreover, in the energy range where the RIA is valid the in-medium NN cross sections are found to increase linearly with density.

Acknowledgement

We thank G. C. Yong and P. Krastev for useful discussions. The work was supported in part by the US National Science Foundation under Grant No. PHY-0652548, the Research Corporation Award No. 7123, the National Natural Science Foundation of China under Grant Nos. 10405031, 10575071 and 10675082, MOE of China under project NCET-05-0392, Shanghai Rising-Star Program under Grant No. 06QA14024, the SRF for ROCS, SEM of China, the Knowledge Innovation Project of the Chinese Academy of Sciences under Grant No. KJXC3-SYW-N2, and the China Major State Basic

Research Development Program under Contract No. 2007CB815004.

-
- [1] I. Tanihata et al., a special volume of Nucl. Phys. **A693**, 1 (2001).
 - [2] L. W. Chen, C. M. Ko, B. A. Li, Phys. Rev. Lett. **94**, 032701 (2005).
 - [3] B. A. Li, L. W. Chen, Phys. Rev. **C72**, 064611 (2005).
 - [4] B. A. Li, P. Danielewicz, W. G. Lynch, Phys. Rev. **C71**, 054603 (2005).
 - [5] T. Gaitanos, C. Fuchs, H.H. Wolter, Phys. Lett. **B609**, 241 (2005).
 - [6] V. Prassa, T. Gaitanos, H. H. Wolter, G. Lalazissis, M. Di Toro, nucl-th/0510035.
 - [7] Y. Zhang, Z. Li, P. Danielewicz, Phys. Rev. **C75**, 034615 (2007).
 - [8] G. Q. Li and R. Machleidt, Phys. Rev. **C 48**, 1702 (1993).
 - [9] G. Q. Li and R. Machleidt, Phys. Rev. **C 49**, 566 (1994).
 - [10] C. Fuchs, A. Faessler, M. El-Shabshiry, Phys. Rev. **C64**, 024003 (2001).
 - [11] F. Sammarruca, P. Krastev, Phys. Rev. **C73**, 014001 (2006).
 - [12] J. Jaenicke, J. Aichelin, N. Ohtsuka, R. Linden, A. Faessler, Nucl. Phys. **A536**, 201 (1992).
 - [13] T. Alm, G. Röpke, M. Schmidt, Phys. Rev. **C50**, 31 (1994).
 - [14] H.-J. Schulze et al., Phys. Rev. **C55**, 3006 (1997); A. Schnell et al., *ibid.*, **C57**, 806 (1998).
 - [15] G. Giansiracusa, U. Lombardo, and N. Sandulescu, Phys. Rev. **C53**, R1478 (1996).
 - [16] M. Kohno, M. Higashi, Y. Watanabe, and M. Kawai, Phys. Rev. **C57**, 3495 (1998).
 - [17] G. Mao, Z. Li, Y. Zhuo, Y. Han, and Z. Yu, Phys. Rev. **C 49**, 3137 (1994).
 - [18] W. H. Dickhoff, C. C. Gearhart, E. P. Roth, A. Polls, and A. Ramos, Phys. Rev. **C 60**, 064319 (1999).
 - [19] Q. Li, Z. Li, and G. Mao, Phys. Rev. **C 62**, 014606 (2000)
 - [20] The Nucleon Optical Potential, Ed. P. E. Hodgson (World Scientific Publishing Co., Singapore, 1994)
 - [21] B. Ter Haar and R. Malfliet, Phys. Lett. **B172**, 10 (1986).
 - [22] J. Rong, Z. Y. Ma, N. V. Giai, Phys. Rev. **C73**, 014614 (2006).
 - [23] N. A. Khokhlov, V. A. Knyr, Phys. Rev. **C73**, 024004 (2006).
 - [24] J. A. McNeil, J. R. Shepard, and S. J. Wallace, Phys. Rev. Lett. **50**, 1439 (1983).
 - [25] J. R. Shepard, J. A. McNeil, and S. J. Wallace, Phys. Rev. Lett. **50**, 1443 (1983).
 - [26] B. C. Clark S. Hama, R. L. Mercer, L. Ray, and B. D. Serot, Phys. Rev. Lett. **50**, 1644 (1983).
 - [27] L.D. Miller, Phys. Rev. Lett. **51**, **1733** (1983).
 - [28] J. A. McNeil, J.R. Shepard, and S.J. Wallace, Phys. Rev. **C27**, 2123 (1983).
 - [29] B.D. Serot and J.D. Walecka, Adv. Nucl. Phys. **16**, 1 (1986); Int. J. Mod. Phys. **E 6**, 515 (1997).
 - [30] W. Z. Jiang, B. A. Li and L. W. Chen, arXiv:0705.1738 [nucl-th], Phys. Lett. **B** (2007) in press; arXiv:0707.2795 [nucl-th].
 - [31] G. E. Brown and M. Rho, Phys. Rev. Lett. **66**, 2720 (1991); *ibid.* nucl-th/0509001; *ibid.* nucl-th/0509002.
 - [32] C. Song, Phys. Rep. **347**, 289 (2001).
 - [33] L. W. Chen, C. M. Ko, B. A. Li, Phys. Rev. **C72**, 064309 (2005).
 - [34] M. Jaminon, C. Mahaux and P. Rochus, Nucl. Phys. **A365**, 371 (1981).
 - [35] A. M. Lane, Nucl. Phys. **35**, 676 (1962).
 - [36] G. Q. Li, R. Machleidt, Y.Z. Zhuo, Phys. Rev. **C48**, 1062 (1993).
 - [37] J. W. Negele, K. Yazaki, Phys. Rev. Lett. **47**, 71 (1981).
 - [38] V. R. Pandharipande, S. C. Pieper, Phys. Rev. **C45**, 791 (1992).
 - [39] G. Q. Li, R. Machleidt, Phys. Rev. **C58**, 1393 (1998); *ibid.* **C58**, 3153 (1998).
 - [40] B. A. Li, C. B. Das, S. D. Gupta, C. Gale, Nucl. Phys. **A735**, 563 (2004).
 - [41] C. Fuchs, H.H. Wolter, Eur. Phys. J. **A30**, 5 (2006).
 - [42] D. P. Murdock, C. J. Horowitz, Phys. Rev. **C35**, 1442 (1987).
 - [43] L.W. Chen, F.S. Zhang, Z.H. Lu, and H.R. Ma, Phys. Rev. **C 64**, 064315 (2001).
 - [44] Introduction to nuclear reactions, C. A. Bertulani, P. Danielewicz, (IOP publishing Ltd., London, 2004)
 - [45] Z. H. Li, L. W. Chen, C. M. Ko, B. A. Li, H. R. Ma, Phys. Rev. **C74** 044613, (2006).
 - [46] B. A. Li, C. M. Ko, W. Bauer, Int. J. Mod. Phys. **E7**,147 (1998).
 - [47] D. Klakow, G. Welke, W. Bauer, Phys. Rev. **C48**, 1982 (1993).
 - [48] B. G. Todd-Rutel, J. Piekarewicz, Phys. Rev. Lett. **95**, 122501 (2005).